Comparison between Experimental, Analytical, and Numerical Methods in Natural Frequencies of the Longitudinal Flight Modes for Small UAVs

M. El-Salamony*, S. Serokhvostov†, A.Epikhin‡, and K.Zaripov§
Moscow Institute of Physics and Technology
Department of Aeromechanics and Flight Engineering
140180, Gagarina street, 16, Zhukovsky, Russia

ABSTRACT

In order to design the good controller for an unmanned aerial vehicle (UAV), an accurate mathematical model of aircraft must be constructed first. Geometry and mass of an aircraft are important factors in flight mechanics and in the calculations of stability and natural frequencies of its flight modes, which are of great importance in controller designing process. In this paper, comparison between the formulae of the large aircrafts applied on small UAVs scale, XFLR5 as a numerical commercial vortex lattice method (VLM) program and experimental data obtained from flight tests is made to investigate their accuracy.

NOMENCLATURE

c	aircraft chord
C_L	airplane lift coefficient in steady state condition
C_{L_α}	variation of airplane lift coefficient with angle of attack
C_{m_α}	variation of airplane pitching moment coefficient with angle of attack
C_{m_q}	variation of airplane pitching moment coefficient with pitch rate
g	gravitational acceleration
I_{xx}	moment of inertia around fuselage axis
I_{yy}	moment of inertia around wing axis
I_{zz}	moment of inertia around normal to X and Y axes
m	aircraft mass
M_α	Pitch angular acceleration per unit angle of attack
$M_{\dot{\alpha}}$	Pitch angular acceleration per unit rate of change of angle of attack
M_q	Pitch angular acceleration per unit pitch rate
M_{T_α}	Pitch angular acceleration per unit angle of attack due to thrust
M_u	Pitch angular acceleration per unit change in speed
$\bar{r_z^2}$	dimensionless MAV radius of inertia along the wing
S	reference area
$_{T_u}$	Pitch angular acceleration per unit change in speed due to thrust
U_1	cruise velocity
X_α	forward acceleration per unit angle of attack
X_u	forward acceleration per unit change in speed
Z_α	vertical acceleration per unit angle of attack
$Z_{\dot{\alpha}}$	vertical acceleration per unit rate of change of angle of attack
Z_q	vertical acceleration per unit pitch rate
Z_{T_u}	forward acceleration per unit change in speed due to thrust
Z_u	vertical acceleration per unit change in speed
θ	pitch angle
μ	dimensionless aircraft density
ρ	air density
ϕ	roll angle
ψ	yaw angle
$\omega_{n,lp}$	natural frequency long mode
$\omega_{n,sp}$	natural frequency short mode

*Email address: elsalamony.mostafa@phystech.edu
†Email address: serokhvostov@phystech.edu
‡Email address: ead_94@mail.ru
§Email address: kamil@zaripov.net

1 INTRODUCTION

Since the UAVs (including mini and micro) are designed according to the procedure used for the large aircrafts, the stability calculations usually also follow the same formulae derived for the large aircrafts, but the geometrical scale is much smaller. So, the forces which affect the UAV change their order of power nonlinearly and some assumptions for the manned aircrafts cannot be valid in our case, and we are to introduce new assumptions which are not valid for the manned ones. The attempts of preliminary investigations were conducted previously [1, 2] and now it is being investigated in more detail.

It is well known from flight mechanics that if any disturbance occurred to the aircraft (as gust wind or control surface deflection) the stable aircraft try to damp this disturbance and return to its initial state in a way similar to mass-damper-spring system; oscillations are to be damped to zero. The aircraft has two longitudinal independent oscillations; short mode and long mode. Short mode oscillation is due to variation of angle of attack and the long mode oscillation is due to speed variation. So we can model these motions as two different simple mass-damper-spring systems. In case of damped vibrations, there are 2 definitions for the frequency; the damped frequency and the undamped / natural frequency. In this paper, the natural frequencies are considered.

In order to design a control system for an aircraft, the main step is to make a mathematical model of flight mechanics for the aircraft. The controller's accuracy depends on the accuracy of the mathematical model with respect to the physical model. Even a simple PID control could be used to make the required response if the mathematical model was accurate enough. The goal of this research is to understand how accurate the calculations based on the traditional formulae with respect to the experimental values are.

In this research, we investigate the formulae and some assumptions of calculating the natural frequencies of the longitudinal short and long modes mentioned by J. Roskam[3], D. Hull[4], and I. Ostoslavsky[5] and compare their results with the numerical VLM calculations from XFLR5 which is mainly designed for small UAVs[6] then these results are compared to real measurements of the natural frequencies obtained from UAV "Sonic 185" at flight.

2 PROCEDURE

For an aircraft, we can model its longitudinal motion as fourth order equation which - under some conditions - can be divided into two second order equations, short and long period modes. Roskam and Ostoslavsky considered this technique but with different procedure. Roskam's procedure[3] -and same for Hull[4] - starts from the aerodynamic coefficients, then calculating the forces on the aircraft then cast them together to create the coefficients of the main characteristic equation. By deep understanding of the physics behind the aircraft forces and their order of magnitude and vibrations, Hull and Roskam have made an approximate solutions for obtaining the natural frequency directly instead of solving the main fourth order equation by linking the forces directly to the natural frequency and damping ratio.

Ostoslavsky has derived the characteristic equation by a different method. Instead of calculating the forces, he used directly the non-dimensional aerodynamic coefficients and cast them together to get the coefficients of the characteristic equation. By deep understanding of the mathematics behind the characteristic equation, he decomposed the fourth order equation into two second order ones, each one describe a single flight mode under the fact that the natural frequency of the short mode is much bigger than the long mode.

In numerical methods as VLM as used in XFLR5 - the aircraft is divided into small panels. For each panel, a normal vector is set to be perpendicular to the camber. Also a combination of source, doublet, and vortex are added in one quarter of the panel, and a control point is added after three quarters of the panel to achieve the no-penetration condition[7]. By solving N equations obtained from the N panels, the total vortex strength is determined then the normal and tangential forces acting on the aircraft are obtained then converting them into non-dimensional coefficients. The next step is to import these values which are depend on the angle of attack - into the state space matrix and obtain the eigen values of the matrix which are a combination of natural frequency and damping ratio and they can be separated easily. XFLR5 is used because it is open source and used widely for UAV design process and also has the ability to obtain the natural frequencies and damping ratios.

Experimental data are obtained from real flight measurements using two different devices; the gyroscope of ArduPilot[8] with low sampling frequency and SmartAP[9] which has higher sampling frequency. Two methods are used in measuring the pitch angle; Euler angles from the gyroscope directly and quaternions to investigate the error between them. More details are in section 4.

2.1 The aircraft

The UAV used in this research is Sonic 185 of DYNAM[10]. Aircraft parameters and geometry are measured and listed in tables 1 and 2.

2.2 Airfoil

There is no data about the airfoils used in the wing and empennage of the airplane investigated. So, it was decided to find nearly similar profile from the known ones. Estimation of the airfoil is based on measurements of the thickness to chord ratio and the position of maximum camber and searching for a similar airfoil. Given that thickness to chord ratio is 10.7% at 39%, this leads to choose the airfoil E231 of Eppler series which shows good convergence as its thickness to chord ratio is 12.3% at 39.4%. For the empennage, NACA 0006 is used.

Property	value
$Mass\ [kg]$	1.183
$I_{xx}\ [kg.m^2]$	0.108
$I_{yy}\ [kg.m^2]$	0.065
$I_{zz}\ [kg.m^2]$	0.122
$Cruise\ velocity\ [m/s]$	8
$Aspect\ ratio$	10.295
$Span\ [m]$	1.85
$Wing\ area\ [m^2]$	0.33
$Center\ of mass\ from\ leading\ edge\ of\ root\ section\ [m]$	0.07

Table 1: Aircraft parameters.

Property	Wing	Horizontal Tail	Vertical Tail
$Aspectratio$	10.295	4.92	2.03
$Rootchord\ [m]$	0.205	0.125	0.2
$Tipchord\ [m]$	0.06	0.02	0.115
$Mean\ chord\ [m]$	0.189	0.1	0.16
$Span\ [m]$	1.85	0.48	0.16
$Area\ [m^2]$	0.33	0.046	0.03
$Sweep\ angle\ from\ Leading\ edge\ [degree]$	6.71	18.17	23.25

Table 2: Sonic 185 geometry.

3 CALCULATIONS

3.1 Aerodynamic coefficients

The aerodynamic and stability coefficients are calculated according to Roskam procedure[11] and the results are shown in table 3. It is noticed that C_{mq} in Roskam formulae is twice the one in Ostoslavsky formulae by definition.

Derivative	Lift coeff.	Drag coeff.	Moment coeff.
α	5.253	0.377	-0.47
q	7.312	0	Roskam:-8.59 Ostoslavsky: -4.295
$\dot{\alpha}$	4.655	0	-4.1337

Table 3: Aerodynamic derivatives

3.2 Roskam and Hull procedure

In this section we will consider the procedure of Roskam (exact and approximate) and Hull together because they have quite similar formulae and results as a sequence.
The characteristic equation of Roskam[3] is

$$Ax^4 + Bx^3 + Cx^2 + Dx + E = 0 \tag{1}$$

where;

$$A = U_1 - Z_{\dot{\alpha}} \tag{2}$$

$$B = (-(U_1 - Z_{\dot{\alpha}})(X_u + X_{Tu} + M_q) - Z_\alpha M_{\dot{\alpha}}(U_1 + Z_q) \tag{3}$$

$$C = (X_u + X_{Tu})[M_q * (U_1 - Z_{\dot{\alpha}}) + Z_\alpha + M_{\dot{\alpha}}(U_1 + Z_q)] + M_q Z_\alpha - Z_u X_\alpha + M_{\dot{\alpha}} g \sin\theta_1 - (M_\alpha + M_{T\alpha})(U_1 + Z_q) \tag{4}$$

$$D = g\sin\theta_1[M_\alpha + M_{T\alpha} - M_{\dot{\alpha}}(X_u + X_{Tu})] + g\cos\theta_1[Z_u M_{\dot{\alpha}} + (Mu + M_{Tu})(U_1 - Z_{\dot{\alpha}})] + (M_u + M_{Tu})[-X_{\dot{\alpha}}(U_1 + Zq)] + Z_u X_\alpha M_q + (X_u + X_{Tu})[(M_\alpha + M_{T\alpha})(U_1 + Z_q) - M_q * Z_\alpha] \tag{5}$$

$$E = g\cos\theta_1[(M_\alpha + M_{T\alpha})Z_u - Z_\alpha(M_u + M_{Tu})] + g\sin\theta_1[(M_u + M_{Tu})X_\alpha - (X_u + X_{Tu})(M_\alpha + M_{T\alpha})] \tag{6}$$

After analysis, the results showed that ω_n=1.0066 Hz for the short mode, and 0.178 Hz for the long mode. It is important to mention that the damping ratio of the short mode is 0.96.
The approximate solution for the natural frequency of the short and long modes according to Roskam are:

$$\omega_{n,sp} = \sqrt{\frac{Z_\alpha * M_q}{U_1} - M_\alpha} \tag{7}$$

$$\omega_{n,lp} = \sqrt{\frac{-Z_u * g}{U_1}} \tag{8}$$

The results are: ω_n=1.0501 Hz for the short mode, and 0.2835 Hz for the long mode.
According to Hull method[4], the approximate formulae for short mode and long mode are

$$\omega_{n,sp} = \sqrt{\frac{Z_\alpha * M_q - M_\alpha * (U_1 + Z_q)}{U_1 + Z_{\dot{\alpha}}}} \tag{9}$$

$$\omega_{n,lp} = \sqrt{\frac{-Z_u * g}{U_1 + Z_q}} \tag{10}$$

The results are quite similar to the approximate Roskam formulae as shown: for short mode,ω_n=0.9888 Hz and for long mode ω_n=0.302 Hz.

3.3 Ostoslavsky procedure

Ostoslavsky method [5] is good method for direct determination of what parameters affect the frequencies. He introduced the characteristic equation of the system as fourth order function in its eigen values as:

$$F = \lambda^4 + a_1\lambda^3 + a_2\lambda^2 + a_3\lambda + a_4 = 0 \tag{11}$$

where the coefficients of this equations under the steady state condition are:

$$a_1 = C_{L\alpha} - \frac{C_{m\dot{\alpha}} + C_{mq}}{\bar{r_z^2}} \tag{12}$$

$$a_2 = \frac{C_{m\alpha} * \mu + C_{L\alpha} * C_{mq}}{\bar{r_z^2}} \tag{13}$$

$$a_3 = \frac{-2C_L[(C_L - C_{D\alpha}) * C_{mq} + C_L * C_{m\dot{\alpha}}]}{\bar{r_z^2}} \tag{14}$$

$$a_4 = \frac{-2C_L^2 * \mu * C_{m\alpha}}{\bar{r_z^2}} \tag{15}$$

and

$$\bar{r_z^2} = \frac{I_{yy}}{m * c^2} \tag{16}$$

$$\mu = \frac{2m}{\rho * S * c} \tag{17}$$

By solving equation (11), we obtain the eigen values of the system which indicate their natural frequencies and damping ratios.
In order to simplify the decomposition of the characteristic equation, Ostoslavsky supposed that the eigen values of the long mode is negligible with respect to the short mode, and finally the natural frequencies of the short and long modes can respectively obtained from:

$$\lambda^2 + a_1\lambda + a_2 = 0 \tag{18}$$

$$\lambda^2 + \frac{a_2a_3 - a_1a_4}{a_2^2}\lambda + \frac{a_4}{a_2} = 0 \tag{19}$$

The results for the exact equation are ω_n = 0.1787 Hz for the long mode but for the short mode the eigen values were real which means that the short mode vibration is over damped. The results of the simplified equations are ω_n=0.1758 Hz for the long mode and the short mode also is over damped.

Another approach is used to identify the natural frequency in this case. It is well known from the definition of the eigen value that:

$$\lambda = -\omega_n * \zeta \pm \sqrt{(\omega_n * \zeta)^2 - \omega_n^2} \tag{20}$$

so the natural frequency can be calculated from the analysis of the left and right parts individually and comparing them with the formula of the roots of the second order equation. Using this 'equation-similarity' approach, the natural frequency is calcuated and the result is 1.0605 Hz. This is close to the result obtained by Roskam procedure.

3.4 XFLR5 Calculations

The UAV is drawn on XFLR5 using the measurements from tables 1 and 2 as shown in figure 1 . It should be noted that there is no fuselage in this model.
Calculation done shows that ω_n=1.129 Hz for the short mode, and 0.178 Hz for the long mode.

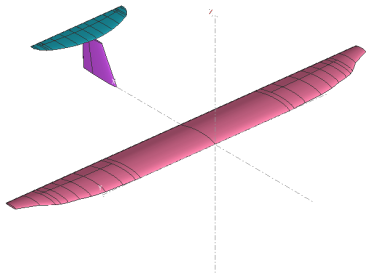

Figure 1: Sonic 185 drawing in XFLR5

3.5 Experiment and Experimental Data

The experiment was conducted for the steady cruise flight of the aircraft with two measuring devices. To prevent the additional disturbances, the plane was controlled in manual mode without autopilot stabilization. During the flight the aircraft was balanced so as it moves straight at the constant altitude and with the constant velocity. Flight parameters were controlled form the ground station of Ardupilot by means of telemetry link.
Two sets of sensors were used independently for more accuracy and doubling the amount of data and also to notice the difference between results for different sampling frequency and different ways to measure flight angles. First set is the data obtained from the gyroscope of the autopilot of type ArduPilot Mega which measure pitch, roll, and yaw angles of the aircraft and has sampling frequency of 3.7 Hz. The second set of data is from SmartAP that can measure with sampling frequency up to 250 Hz and use quaternions which provide a convenient mathematical notation for representing rotations and orientations of objects in three dimensions. It has some benefits compared to Euler angles; they are simpler to compose and avoid the problem of gimbal lock. Compared to rotation matrices they are more numerically stable and efficient[12].
In order to convert quaternions to pitch, roll, and yaw, transformation of equation (21) [13] is used. Quaternions and their equivalent Euler angles are shown in figures 2 and 3 respectively.

$$\begin{pmatrix} \phi \\ \theta \\ \psi \end{pmatrix} = \begin{pmatrix} \tan^{-1}\frac{2(q_0q_1+q_2q_3)}{1-2(q_1^2+q_2^2)} \\ \sin^{-1}2(q_0q_2 - q_1q_3) \\ \tan^{-1}\frac{2(q_0q_3+q_1q_2)}{1-2(q_1^2+q_2^2)} \end{pmatrix} \tag{21}$$

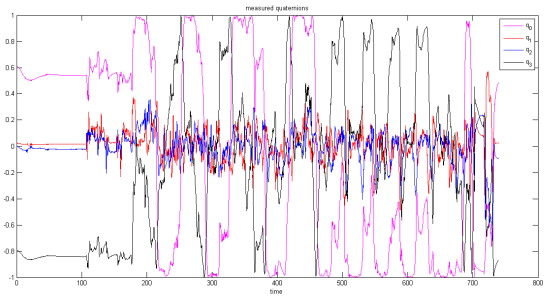

Figure 2: Quaternions estimated during flight.

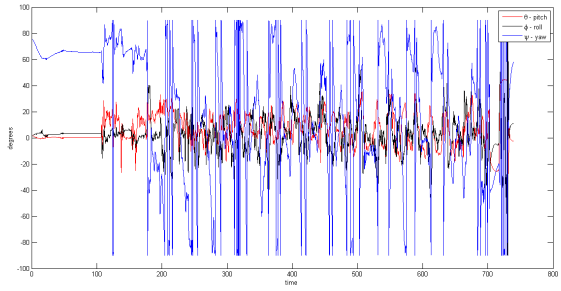

Figure 3: Euler angles calculated from quaternions.

Both data sets retrieved are processed by Fast Fourier Transform[14] once without filter and another time with filter. While examining the signal without filter, it is taken into account the signal first and last points have the same values to prevent aliasing as illustrated in figure 4.

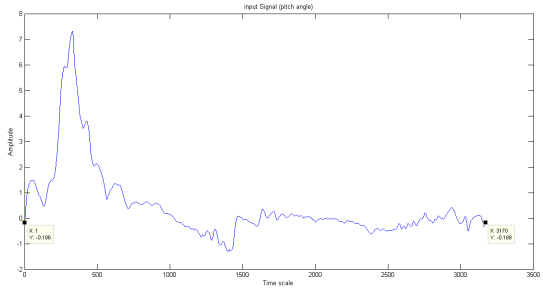

Figure 4: Sample for a signal which first and last points have the same values to prevent aliasing.

Data are filtered by Hanning filter[15, 16] to prevent leakage in the transform[17]. Such filter is chosen for this case because:

1. we are investigating a random signal with unknown frequency.
2. the vibrations are within narrow band.
3. the exact amplitude is not as important as the value of the frequency itself.
4. overcome the noise and get the mean value of the frequency.

For these four reasons, the most suitable filter is Hanning filter[17]. Data signal of pitch angle are shown in figure 5.

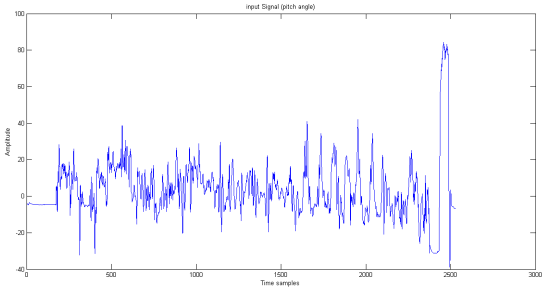

Figure 5: Pitch angle during flight.

Fast Fourier Transform -or simply FFT- is used to convert discrete time samples from time to frequency domain. After processing and filtering, some frequencies appeared close to each other with comparable amplitudes. After some averaging, the results show a freq of 0.18±0.01 Hz. Vibrations due to motor are not captured because its frequency is rather high but it act at noise all over the signal. Figures 6 to 8 show samples of the obtained results at different periods of time.

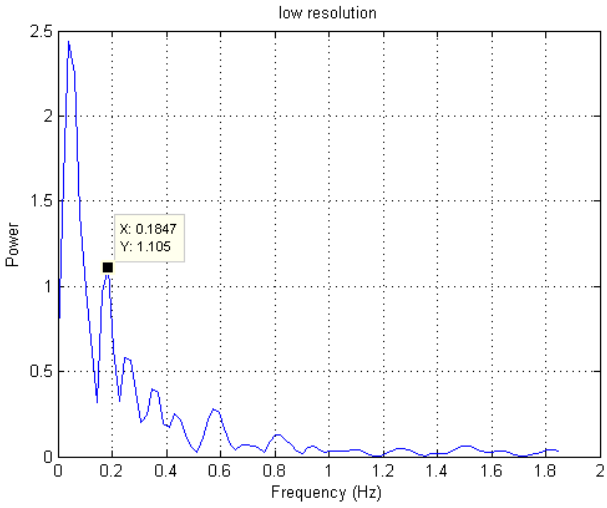

Figure 6: Sample 1 of the processed signal .

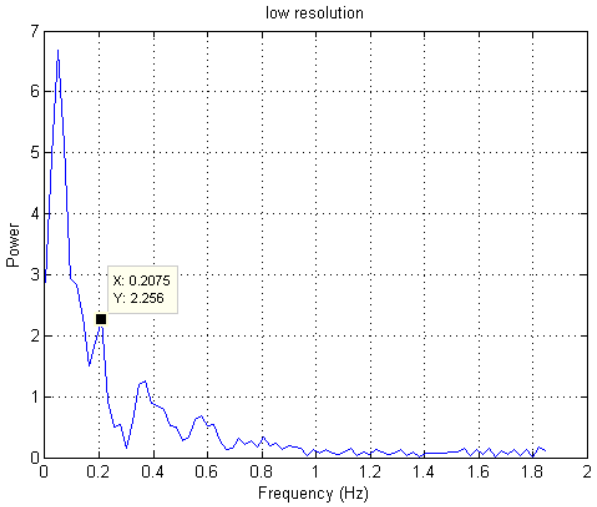

Figure 7: Sample 2 of the processed signal .

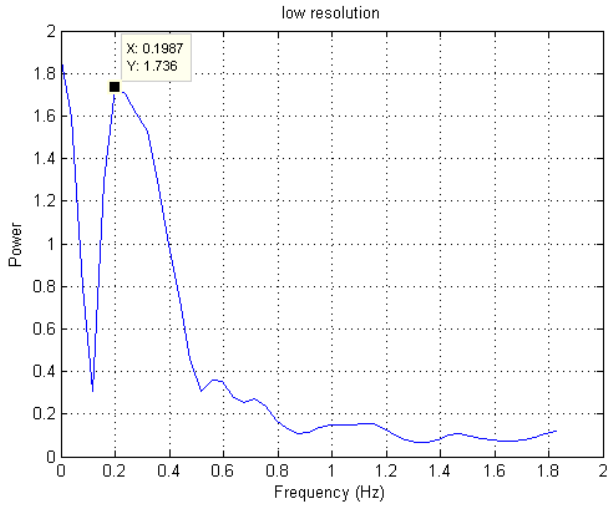

Figure 8: Sample 3 of the processed signal .

4 Analysis and Discussion

Concerning the mismatch of C_{mq} definition between Roskam and Ostoslavsky, although this conflict may be a problem but the C_{mq} used in the formula of Roskam for the natural frequency is divided by factor of 2, so the result is the same as Ostoslavsky. This shows that every procedure must follow its own definition for the aerodynamic and stability coefficients.

It is noticed that approximate methods of Roskam and Hull overestimate the long mode frequency. This is because they neglected some terms under the assumption that μ -which indicates the mass of the aircraft - is rather big compared to $C_{L\alpha} * C_{mq}$ but this condition is not applicable in the UAVs.

Considering the devices used in the experimental measurement, the low-frequency device could not measure frequencies more than 2 Hz because it need more sampling frequency. The signal of the pitch angle from the gyroscope and the transformed one are quite similar as shown in figure (9) except in the peak points since the high frequency device can capture it better.

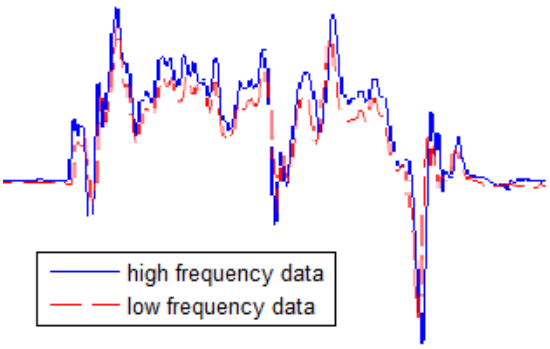

Figure 9: Sample from both signals together.

By comparing the calculations with the experimental results (table 4), it is obvious that the long mode frequencies obtained from Roskam exact formula, Ostoslavsky formulae and XFLR5 are within the allowable region of the experimental result. For the short mode frequency, Ostoslavsky method shows that this motion has no oscillations, Roskam methods also shows that the damping ratio is 0.96, so even if it exists, it will be rather difficult to be observed since the damping ratio decrease the amplitude in the frequency domain. In order to clarify this point, this problem will be considered again with additional calculations and measurements.

Method	Short	Long
Roskam - exact	1.0066	0.178
Roskam - approx	1.0501	0.2835
Hull (approx)	0.9888	0.302
Ostoslavsky - exact	–	0.1787
Ostoslavsky - approx	1.0605[1]	0.1758
XFLR5	1.12	0.178
experiment	–	0.18 ± 0.01

Table 4: Results of natural frequencies of all methods.

. Regarding the assumption of that the long mode frequency is much lower than the short mode frequency, these two frequencies obtained from the results are compared

[1] using the 'equation-similarity' approach in subsection 3.3

to each other. In Roskam case, the long mode frequency is 17.7% of the short mode. In XFLR5, long mode frequency is 15.9% of the short mode so we can conclude that the assumption of short mode is much bigger than the long mode is valid for small UAVs.

5 Conclusion

This research compares the natural frequencies of longitudinal motion calculated by the usual methods of estimation for the manned aircrafts found in the references of Roskam, Hull, and Ostoslavsky, and the numerical VLM program XFLR5 with experimental values of real flight measured by two different devices with different sampling frequencies and methods of measuring the angles. It is found that there is no dependence of the experimental data on the method of measuring the flight angles or on sampling frequency. The assumption of long mode can be neglected with respect to the short mode is valid. For the long mode, exact Roskam, Ostoslavsky, and XFLR5 estimate the frequency within range of the experimental results while the methods of Roskam approximation and Hull are not correct in case of small UAVs. As for the short mode, we encountered the situation that our data are near the critical point and a set of additional analysis and experiments must be provided. It is noted that results from analytical methods are valid only for the aerodynamic coefficients defined in the same procedure.

Acknowledgement

The first author acknowledge the scholarship for masters degree from Moscow Institute of Physics and Technology (MIPT) for international students.

References

[1] S.V. Serokhvostov, A.A.Dementyev, and T.E. Churkina. Analytical investigation of mav dynamical characteristics and its influence on design. In *proc of International Micro Air Vehicle Conference (IMAV), Braunschweig, Germany*, 2010.

[2] S.V. Serokhvostov, N. Pushchin, and K. Shilov. Mav unsteady characteristics in-flight measurement with the help of smartap autopilot. In *proc of International Micro Air Vehicle Conference (IMAV), Toulouse, France*, 2013.

[3] Jan Roskam. *Airplane flight dynamics and automatic flight controls*. DARcorporation, 1995.

[4] David G Hull. *Fundamentals of airplane flight mechanics*. Springer, 2007.

[5] I.V. Ostoslavsky. Aerodynamics of aircraft. *Oborongiz, Moscow*, 1957.

[6] André Deperrois. XFLR5 analysis of foils and wings operating at low Reynolds numbers. *Guidelines for XFLR5*, 2009.

[7] Edward Lewis Houghton and Peter William Carpenter. *Aerodynamics for engineering students*. Butterworth-Heinemann, 2003.

[8] ardupilot dev Team. Archived:apm 2.5 and 2.6 overview. `http://ardupilot.org/copter/docs/common-apm25-and-26-overview.html`, 2015. last accessed april,2016.

[9] Smart AutoPilot. smartap autopilot manual. `http://sky-drones.com/content/10-manuals`, 2015. last accessed april,2016.

[10] Universal Power Enterprizes Ltd. *Sonic 185: Instruction manual.* Universal Power Enterprizes Ltd., Kowloon, Hong Kong, 2008.

[11] Jan Roskam. *Methods for estimating stability and control derivatives of conventional subsonic airplanes*. DARcorporation, 1971.

[12] William Rowan Hamilton. Ii. on quaternions; or on a new system of imaginaries in algebra. *The London, Edinburgh, and Dublin Philosophical Magazine and Journal of Science*, 25(163):10–13, 1844.

[13] James Diebel. Representing attitude: Euler angles, unit quaternions, and rotation vectors. *Matrix*, 58(15-16):1–35, 2006.

[14] Richard S Figliola and Donald Beasley. *Theory and design for mechanical measurements*. John Wiley & Sons, 2015.

[15] Tim Wescott. Sampling: What nyquist didnt say, and what to do about it. *Wescott Design Services, Oregon City, OR*, 2010.

[16] L Dactron. Understanding fft windows. *Application Note. lds group*, 2003.

[17] Pierre Wickramarachi. Effects of windowing on the spectral content of a signal. *Sound and Vibration*, 37(1):10–13, 2003.